

Reassessment of marker genes in human induced pluripotent stem cells for enhanced quality control

Received: 16 November 2023

Accepted: 23 September 2024

Published online: 02 October 2024

 Check for updates

Jochen Dobner¹, Sebastian Diecke², Jean Krutmann^{1,3},
Alessandro Prigione⁴ & Andrea Rossi¹✉

Human induced pluripotent stem cells (iPSCs) have great potential in research, but pluripotency testing faces challenges due to non-standardized methods and ambiguous markers. Here, we use long-read nanopore transcriptome sequencing to discover 172 genes linked to cell states not covered by current guidelines. We validate 12 genes by qPCR as unique markers for specific cell fates: pluripotency (*CNMD*, *NANOG*, *SPPI*), endoderm (*CER1*, *EOMES*, *GATA6*), mesoderm (*APLNR*, *HAND1*, *HOXB7*), and ectoderm (*HES5*, *PAMRI*, *PAX6*). Using these genes, we develop a machine learning-based scoring system, “hiPSCore”, trained on 15 iPSC lines and validated on 10 more. hiPSCore accurately classifies pluripotent and differentiated cells and predicts their potential to become specialized 2D cells and 3D organoids. Our re-evaluation of cell fate marker genes identifies key targets for future studies on cell fate assessment. hiPSCore improves iPSC testing by reducing time, subjectivity, and resource use, thus enhancing iPSC quality for scientific and medical applications.

Human induced pluripotent stem cells (iPSCs) are versatile to study and model disease, with the potential for therapeutic applications in personalized regenerative medicine^{1,2}. They can be obtained by reprogramming patient-derived somatic cells with pluripotency factors, yielding cells with embryonic stem cell-like features^{3–5}. These iPSCs can undergo genetic modifications, e.g., by CRISPR/Cas, facilitating patient-specific disease modeling, drug screening, and potentially enabling treatment with patient cells manipulated *ex vivo*^{6–11}. Quality control of iPSCs is essential to ensure their robustness, functional integrity, and safety, which are crucial for rigorous scientific investigations and translational applications¹². Quality control measures include assessment of morphology, nuclear and mitochondrial genome integrity, and pluripotency, i.e., their capability to differentiate into the three primary germ layers endoderm, ectoderm, and mesoderm^{13,14}.

Increasing attention is being paid to genome integrity, with ongoing development of novel approaches^{13,15,16}. When it comes to assessing pluripotency, however, despite efforts to provide guidelines,

researchers are faced with an overwhelming combination of methods and markers to choose from refs. 14,17,18.

First described in the 1970s, the formation and spontaneous differentiation of embryoid bodies (EBs) remains one of the most frequently used tests to assess pluripotency in iPSCs due to its ease of execution and low cost¹⁹. Another method to assess pluripotency is the teratoma assay, which is based on the spontaneous tumor formation of transplanted iPSCs into immunocompromised mice²⁰. Handling mice, however, is cost- and administration-extensive, and such tests unnecessarily involve animal harm, which raises ethical concerns²¹. A major disadvantage of both the EB and the teratoma approach is their stochastic nature: for each experimental replicate, different ratios of differentiated cells are obtained²².

Directed trilineage differentiation provides an alternative to assess pluripotency by employing defined media and has the potential for standardization²¹. It has further been reported that iPSC lines failing the EB-based differentiation assay are in fact able to differentiate into the respective germ layers by directed trilineage differentiation¹².

¹Genome Engineering and Model Development Lab (GEMD), IUF—Leibniz Research Institute for Environmental Medicine, Düsseldorf, Germany. ²Max Delbrück Center for Molecular Medicine (MDC), Berlin, Germany. ³Medical Faculty, Heinrich Heine University Düsseldorf, Düsseldorf, Germany. ⁴University Hospital Düsseldorf, Düsseldorf, Germany. ✉e-mail: andrea.rossi@iuf-duesseldorf.de

Except in the case of the teratoma assay, which involves immunohistochemistry, detection of germ layer-differentiated cells is most often performed by immunofluorescent (IF) imaging or flow cytometry. Although these methods enable single-cell-scale detection of differentiated cells, they require substantial hands-on time, meticulous marker selection, and the implementation of appropriate controls. Furthermore, the absence of established thresholds and reporting guidelines in pluripotency testing renders standardization nearly impossible. Quantitative real-time PCR (qPCR) is a standardized method²³ to detect levels of gene transcripts with high specificity and sensitivity, rendering it a suitable choice to assess pluripotency by analysis of differentiation-specific marker genes.

Despite the potential of directed trilineage differentiation in combination with qPCR-based marker gene assessment to achieve standardization in iPSC pluripotency testing, EB-based spontaneous differentiation is still widely used. This may in part be attributable to the fact that the current version of the “Standards for Human Stem Cell Use in Research” document published by the International Society for Stem Cell Research (ISSCR) contains a “Reduced marker gene set used for [EB] analysis” but not for directed trilineage differentiation¹⁷. In line with this, commercially available qPCR-based solutions to assess pluripotency are specifically tailored to spontaneous EB differentiation and have not been frequently reassessed or further developed^{24,25}. In addition, marker genes to assess iPSC differentiation states have been mainly identified using short-read next-generation sequencing or microarrays and have not been reassessed by third-generation sequencing technologies, which have been reported to detect different transcripts^{26–29}. Reassessment of pluripotency/differentiation markers is therefore warranted to reassure the practical use of marker gene recommendations. Potential overlaps of gene expression patterns between differentiation states are also an obstacle for unequivocal identification of differentiation states, highlighting the need for validated streamlined gene markers^{30–32}.

Here, we reassess markers to identify undifferentiated and differentiated states of iPSCs. We perform long-read nanopore transcriptome sequencing on trilineage-differentiated iPSCs and their undifferentiated counterparts. Our study uncovers three main findings: (1) identification of 172 genes potentially associated with differentiation states not addressed in current guidelines. (2) Discovery that markers recommended for EB formation-based analysis are not directly applicable for evaluating trilineage-differentiated iPSCs using existing protocols. (3) Validation of 12 genes to reliably identify undifferentiated iPSCs and their differentiation states into primary germ layers obtained through directed trilineage differentiation.

Using these genes, we develop the machine learning-based scoring system “hiPSCore”. We train hiPSCore with 15 different iPSC lines and validate its performance with an additional 10 iPSC lines. We further demonstrate that hiPSCore accurately classifies undifferentiated and differentiated iPSCs, predicting their potential to differentiate into specialized 2D cells and 3D organoids. In summary, our study re-evaluates markers suitable for distinguishing undifferentiated and differentiated states of iPSCs, unveiling genes previously not used in this context and demonstrating their utility in pluripotency testing. Through comprehensive analysis and the development of the hiPSCore scoring system, we provide a standardized approach to enhance the accuracy and efficiency of iPSC characterization, laying a foundation for advancements in disease modeling and regenerative medicine.

Results

Assessment of recommended marker genes

To establish a standardized pipeline for the classification of iPSC differentiation states based on qPCR, we assessed markers following directed trilineage differentiation.

First, we established a baseline ground truth standard by employing two commercially available directed trilineage

differentiation kits in parallel. We then monitored the success of directed trilineage differentiation by analyzing 15 different commercially available, reprogrammed, and in-house genome-edited iPSC lines (Supplementary Table 1) using flow cytometry (Fig. 1a). All iPSC lines used in this study displayed high levels of undifferentiated state markers (median Oct3/4: 99.6%, median SSEA-4: 99.8%, Fig. 1b and Supplementary Fig. 1). Following directed trilineage differentiation by two commercially available kits, we measured high levels of endoderm (median CXCR4: 99.6%, median SOX17: 95.3%, Fig. 1c and Supplementary Figs. 2, 3), ectoderm (median PAX6: 96.5%, median SOX2: 99.2%, Fig. 1d and Supplementary Figs. 4, 5), and mesoderm markers (median CD140b: 77.5%, median T/BRACHYURY: 94.4%, Fig. 1e and Supplementary Figs. 6, 7), indicating successful differentiation in our hands.

Next, we aimed to identify a set of marker genes to be used in a standardized qPCR-based pluripotency assay. Initially, we consulted marker recommendations, including the ISSCR guidelines^{14,17,25,33} and analyzed several recommended genes to assess undifferentiated and differentiated states of iPSCs. To benchmark the expression of the selected genes, we started to analyze their expression patterns in the 15 different iPSC lines described before that underwent directed trilineage differentiation with two distinct commercially available kits. Unexpectedly, we encountered several issues when using some of the recommended markers to assess germ layer differentiation. We found overlapping expression patterns among markers recommended for the undifferentiated state (*GDF3*: considerable overlap between undifferentiated iPSCs and endoderm, *SOX2*: considerable overlap between undifferentiated iPSCs and ectoderm), ectoderm (*OTX2*: considerable overlap between ectoderm and endoderm), and mesoderm (*NCAM1*: considerable overlap between mesoderm and ectoderm) (Fig. 1f). To clarify whether our selection of genes was simply unfortunate, we randomly selected genes from the ISSCR marker recommendations and analyzed their gene expression signatures in a set of iPSC lines undergoing directed trilineage differentiation (Supplementary Fig. 8). In line with our previous results, these markers were largely not able to unequivocally discriminate between individual differentiation states. On the other hand, some of the promising-looking candidates are listed as markers for more than one germ layer. Taken together, these findings emphasize (1) the necessity of identifying and validating markers capable of accurately distinguishing between iPSC differentiation states, and (2) the importance of exercising caution when applying marker recommendations to evaluate iPSC differentiation states, particularly for samples not derived from EB-based spontaneous differentiation.

Identification of suitable marker genes by long-read sequencing

To identify robust, potentially unreported markers, we performed Oxford Nanopore Technologies (ONT) long-read transcriptome sequencing on undifferentiated iPSCs and those differentiated into endoderm, ectoderm, and mesoderm by directed trilineage differentiation (Fig. 2a). Variability between replicates was low as assessed by principal component analysis (Fig. 2b). Moreover, gene sets of the respective primary germ layers were significantly upregulated compared to the undifferentiated samples as determined by gene set enrichment analysis (Supplementary Table 2), indicating robust reproducible differentiation dynamics. In line with the results obtained by qPCR, gene expression signatures of the markers listed in the current ISSCR guideline’s recommendations were strongly overlapping between differentiation states (Fig. 2c). For all differentiation states, including the undifferentiated state, the analyzed genes demonstrated little to no exclusivity.

Driven by these findings, we performed a thorough analysis of long-read sequencing data to identify markers with enhanced potential to discriminate between all four differentiation states (each

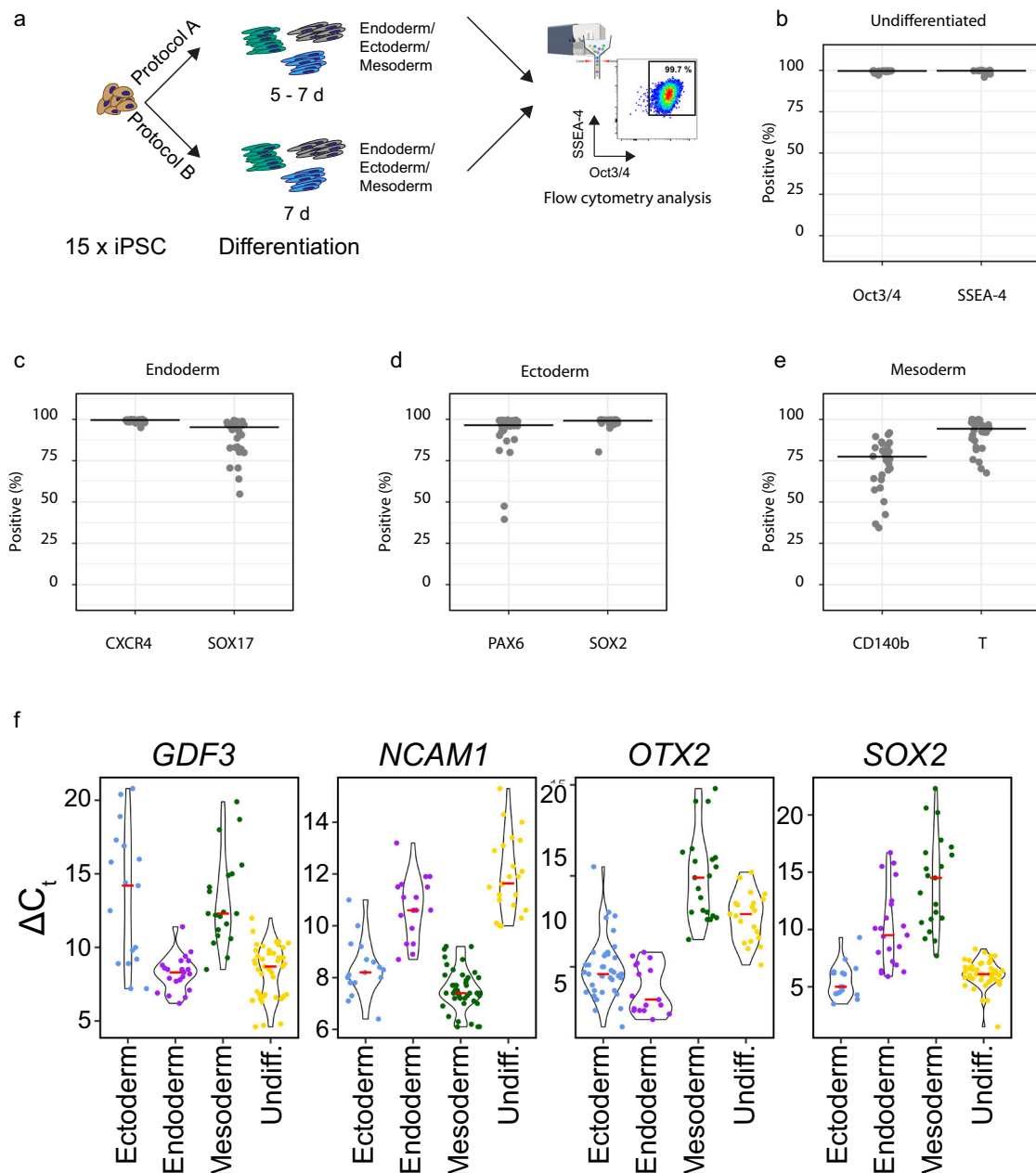
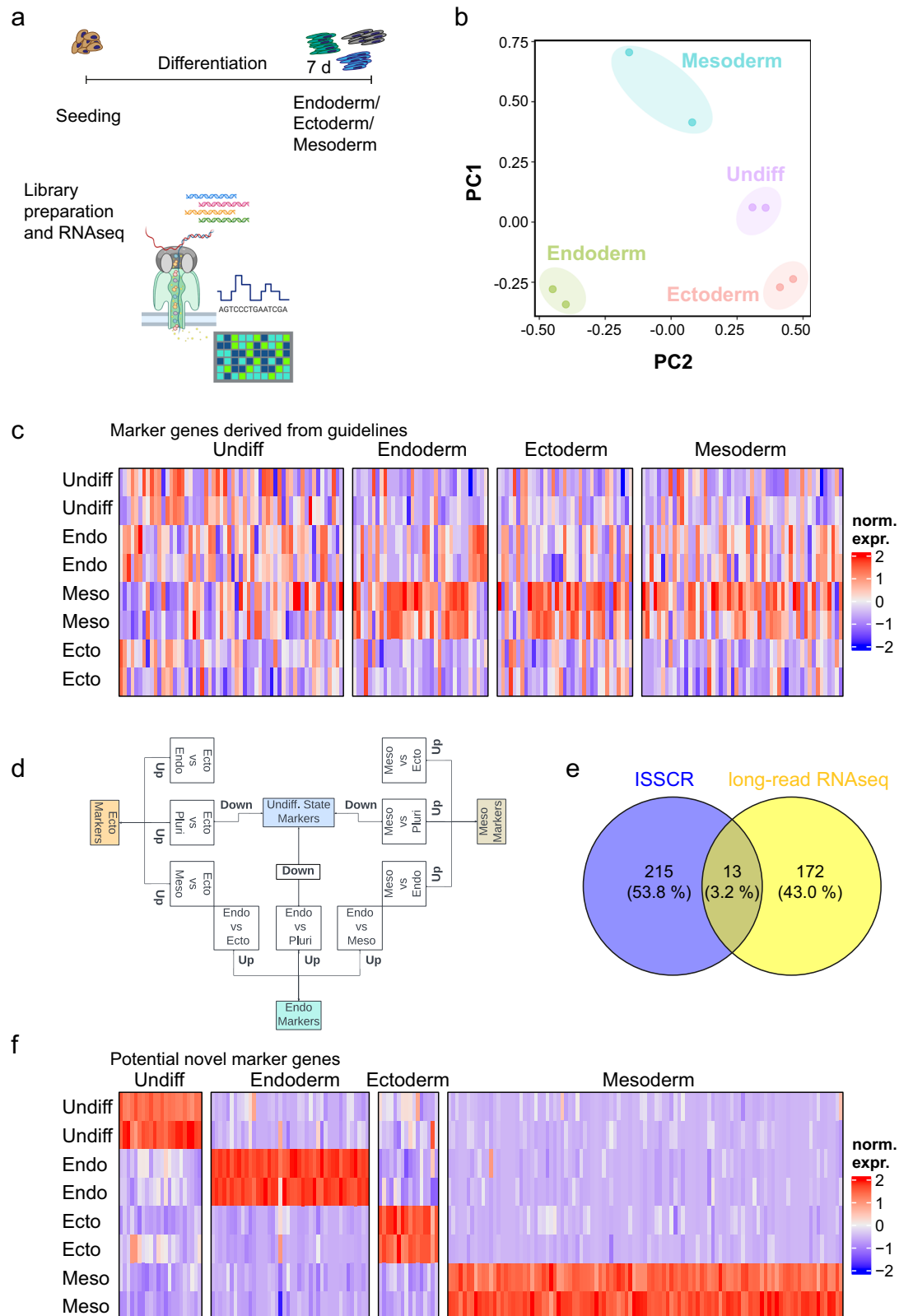


Fig. 1 | Characterization of undifferentiated and trilineage-differentiated human induced pluripotent stem cells. **a** Human induced pluripotent stem cells (iPSCs) were differentiated into the three primary germ layers endoderm, ectoderm, and mesoderm by two different commercially available kits (Protocol A: STEMCELL Technologies, Protocol B: Miltenyi Biotec). Undifferentiated starting iPSC populations and differentiated samples were analyzed by flow cytometry to determine **b** initial purity of the used cells ($n = 15$ independent iPSC lines) and the success of germ layer differentiation into **c** endoderm, **d** ectoderm, and **e** mesoderm. For (**c–e**), $n = 15$ independent iPSC lines were differentiated by each Protocol A and B, totaling 30 independent samples per germ layer. The flow cytometry plot in (**a**) shows the marker analysis for the undifferentiated state

markers Oct3/4 and SSEA-4 as an example. **f** In qPCR, the commonly used markers of the undifferentiated state *GDF3* and *SOX2* display overlapping expression patterns between the analyzed undifferentiated iPSC samples and germ layer-differentiated iPSC samples, whereas the ectoderm marker *OTX2* cannot be used to discriminate between ectoderm/endoderm and mesoderm/undifferentiated states. The mesoderm marker gene *NCAM1* shows overlapping expression patterns between mesoderm and ectoderm. For each gene >100 data points were analyzed. ΔC_t : normalized (to *ACTB* and *GAPDH*) gene expression of analyzed samples. In (**a**), the flow cytometry device icon was created with BioRender.com released under a Creative Commons Attribution-NonCommercial-NoDerivs 4.0 International license.

of the three primary germ layers plus the undifferentiated state, Fig. 2d). With this strategy, we identified 185 genes with strong potential to serve as unequivocal markers to discriminate between differentiation states (Fig. 2e, f). Notably, these markers showed only minimal overlap (13 genes, 3.2%) with the 228 genes of the ISSCR guidelines detected with ONT sequencing (Fig. 2e). When comparing 247 publicly available datasets of undifferentiated iPSCs, we identified distinct patterns between short- and long-read sequencing

(Supplementary Fig. 9a). These divergent gene expression signatures include some markers for undifferentiated iPSCs previously not used for this purpose. We identified five of these genes of interest with distinct expression patterns between short- and long-read sequencing data (Supplementary Fig. 9b). In summary, we identified a set of 172 genes not included in the current ISSCR guidelines with the potential to unequivocally discriminate between the four differentiation states (Fig. 2e, f).



Validation of marker genes to identify differentiation states

Gene expression signatures detected by transcriptome sequencing are not always directly transferable to qPCR-based measurements^{34,35}. On the other hand, data from the literature suggest potential iPSC differentiation marker genes that were not detected in our transcriptome sequencing, potentially due to the higher sensitivity of qPCR-based approaches. By integrating our transcriptome sequencing data,

reports from the literature, and initial testing of promising targets, we selected a total of 14 genes (three per germ layer plus two reference genes) with high potential to unequivocally identify each of the four differentiation states (Supplementary Table 3). Twelve genes were selected for the identification of a specific differentiation state, three for each undifferentiated iPSC (*CNMD*, *NANOG*, *SPPI*), endoderm (*CER1*, *EOMES*, *GATA6*), ectoderm (*HESS*, *PAMR1*, *PAX6*), and mesoderm

Fig. 2 | Long-read nanopore transcriptome sequencing identifies distinct gene expression patterns. **a** Long-read nanopore transcriptome sequencing of two biological replicates of undifferentiated control human induced pluripotent stem cells (iPSCs) and iPSCs differentiated into the three primary germ layers endoderm, ectoderm, and mesoderm. **b** Principal component (PC) analysis demonstrates low variability between experiments and pronounced differences between iPSC differentiation states. **c** Marker genes derived from the 2023 International Society for Stem Cell Research (ISSCR) guidelines show high homogeneity among differentiated samples and are not feasible to unequivocally characterize the analyzed

samples. **d** The described strategy to identify suitable marker genes is based on unique gene expression profiles between differentiation states. **e** Venn Diagram showing the low (3.2%) overlap between marker genes of the current (2023) ISSCR guidelines and marker genes identified in this study. **f** The scaled heatmap of log₂ counts per million-normalized samples indicates clearly distinct gene expression patterns between the samples, supporting their potential suitability as unequivocal markers of distinct iPSC differentiation states. In (a), the nanopore sequencing scheme was created with BioRender.com released under a Creative Commons Attribution-NonCommercial-NoDerivs 4.0 International license.

(*APLN*, *HAND1*, *HOXB7*). Two additional genes were selected as reference genes (*ACTB*, *GAPDH*). To verify the potential use of this gene panel in a standardized qPCR-based assay, we performed a thorough validation by analyzing their gene expression profiles in 15 different iPSC lines differentiated by two different commercially available kits (Figs. 1 and 3a and Supplementary Table 1). We analyzed the gene expression levels for each of the target genes and obtained distinct gene expression signatures for each individual sample. By performing correlation analysis, we observed high similarities between samples (Fig. 3b), indicating that the validated genes may potentially be used to unequivocally identify each of the four differentiation states. When looking at the selected genes individually, we found that each gene set of three genes had the power to discriminate between the undifferentiated state (Fig. 3c), endoderm (Fig. 3d), ectoderm (Fig. 3e), and mesoderm (Fig. 3f). Next, we considered implementing a supervised machine learning-based classification scoring system. Such systems are proficient at identifying patterns in complex datasets and provide accurate and unbiased automated predictions. To test this assumption, we used a total of 105 individual samples (15 iPSC lines each differentiated into each of the 3 primary germ layers with 2 different commercially available kits) comprising a total of 1260 data points (12 genes normalized using two reference genes per sample) to train a machine learning-based classifier (for details see “Methods” section). Specifically, the task of this classifier was to predict the differentiation state of each individual sample by taking normalized qPCR-derived ΔC_t values of all 12 genes per sample into account. We tested several models that demonstrated high predictive power to classify the differentiation state of the analyzed samples (Fig. 3g). The tested models showed high receiver operating characteristic (ROC) area under the curve, precision, sensitivity, and specificity, supporting the feasibility of our gene set to be used to assess iPSC quality in a directed trilineage differentiation approach. Next, we sought to gain insights into the gene expression dynamics and to determine the optimal timepoint for analysis during directed trilineage differentiation. Thus, we analyzed the temporal expression in a subset of three different iPSC lines (Supplementary Fig. 10a). We found that endodermal and mesodermal genes are upregulated after 2–3 days and remain elevated until day 5, while ectodermal genes are upregulated only after 5–7 days (Supplementary Fig. 10b–f). Therefore, we concluded that the optimal data point for analysis would be after 5 (endoderm, mesoderm) to 7 (ectoderm) days of differentiation.

Development of the hiPSCore classification algorithm

We leveraged these findings and developed a classification algorithm named “hiPSCore” to enable standardization of iPSC pluripotency testing. Broad usage of a classification scoring system is facilitated by ease-of-use, high reproducibility, a high degree of robustness, and the potential to be strengthened by samples to be tested in the future. In addition, the number of analyzed transcripts should be streamlined to maximize sample throughput. To account for these points, we developed hiPSCore to enable reproducible classification of iPSC-derived samples. We made use of the 1260 normalized ΔC_t values generated by qPCR analysis of the sub-selection of three marker genes per germ layer (Fig. 3 and Supplementary Table 3). Based on directed trilineage differentiation and analyzed flow cytometry data (Fig. 1), samples were

classified as “0” when they were not differentiated into a specific state of interest and “1” when they were. For instance, a mesoderm-differentiated sample was classified as “1” for mesoderm marker gene expression and as “0” for each undifferentiated, endoderm, and ectoderm marker gene expression. Each subset of three genes selected for each differentiation state showed clearly distinguishable expression patterns between “0” and “1” classes (Figs. 3b–e and 4a–d). To streamline the analysis and increase multiplexing capacity, we aimed to develop a classification score based on the assessment of each differentiation state with its corresponding marker gene set individually. By using the ΔC_t rather than fold-change, the use of a universal control group run on every qPCR plate becomes obsolete. Furthermore, implementation and testing of the workflow on virtually any qPCR device is easily achievable.

To find the best model for predicting the quality of the analyzed samples, we employed the dummy-coded binary variables (“0”/“1”) described before. We then tested different machine learning-based models (for details, see “Methods” section) to identify the model with the highest predictive accuracy and specificity for each differentiation state (Fig. 4e–h). Due to the sophisticated selection and validation of marker genes, the final models were able to unequivocally classify samples in up to 100% of the cases, regardless of the differentiation state analyzed (Fig. 4e–h).

Results of each individual subtest are integrated by multiplying the classification score for each differentiation state with the certainty of classification p , yielding a continuous final hiPSCore quality score (hQS) with: ≥ 3 : pass, ≥ 2 : warning, < 2 : fail. The hQS can be reported, enabling easy sharing of quality assessment across laboratories and cell lines. A given sample will only pass the test if it passes all four subtests, ensuring that only truly pluripotent samples will pass.

To rule out overfitting, we benchmarked the individual germ layer subtests with a test set consisting of 10 additional iPSC lines derived from externally trilineage-differentiated iPSCs. A total of 30 samples (10 per endoderm, ectoderm, and mesoderm), for which corresponding flow cytometry data were available, were analyzed with each specific subtest. For all samples, the individual hiPSCore subtests were passed successfully (Supplementary Table 4), indicating that our classification algorithm is robust to identify directed trilineage-differentiated iPSC-derived samples independent from individual laboratory setups.

Applicability of the hiPSCore classification algorithm

To explore potential cost-saving benefits and tailored experimental design, we tested custom differentiation protocols. Building upon our hiPSCore classification approach, we evaluated its adaptability to custom protocols by examining growth factor- and small molecule-based directed differentiation methods across three different iPSC lines (Fig. 5a). For all three cell lines, the germ layer-specific test was passed for mesoderm (Fig. 5b), endoderm (Fig. 5c), and ectoderm (Fig. 5d), indicating that the identified marker genes can be robustly applied to a broader range of directed trilineage differentiation protocols.

We then aimed to demonstrate the real predictive value of our developed hiPSCore as a pluripotency test by subjecting iPSCs to differentiation in both 2D cell systems and 3D organoids. This approach

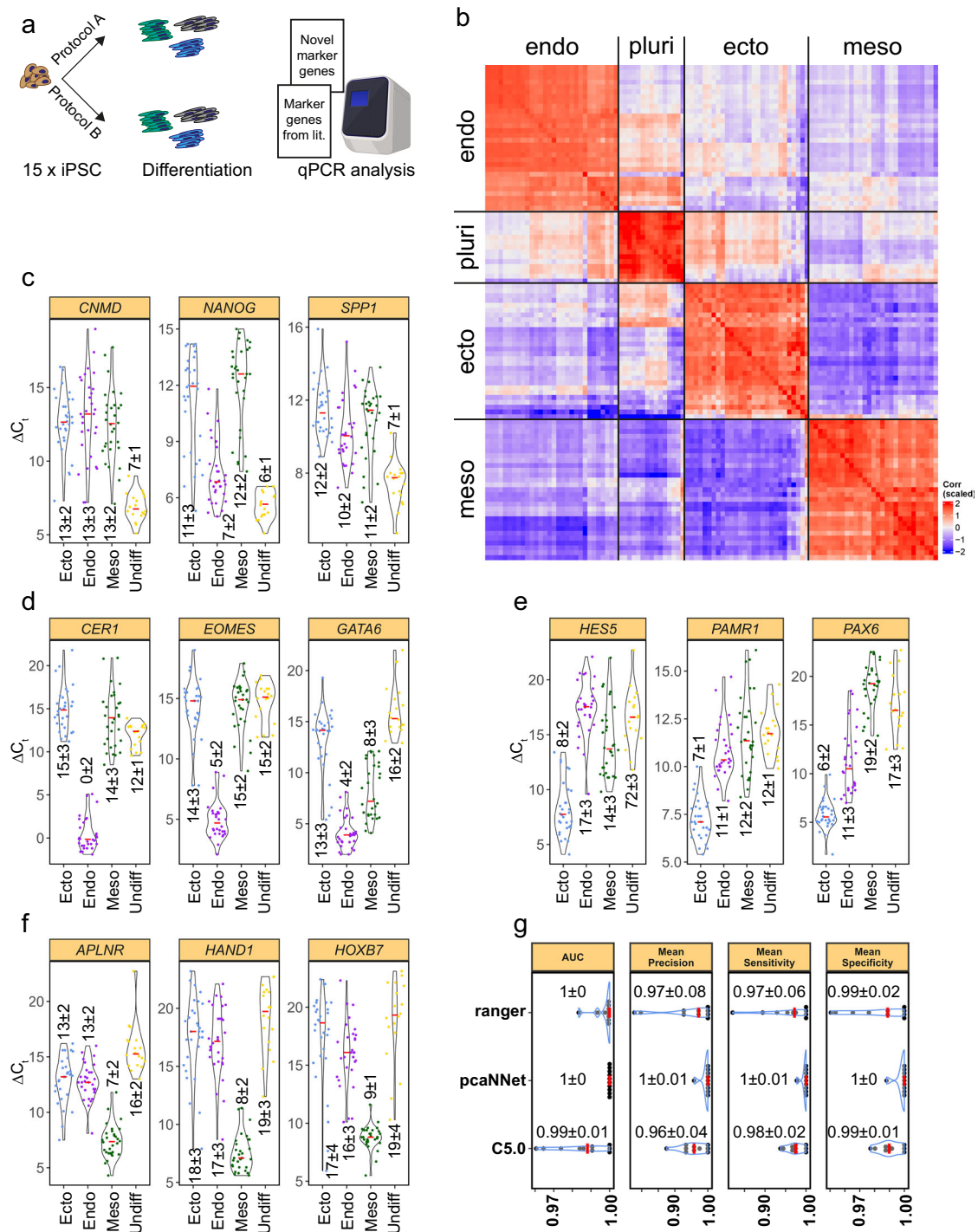


Fig. 3 | Validation of lineage-specific target genes by qPCR. **a** Potential marker genes identified by long-read transcriptome sequencing were validated by qPCR-based gene expression analysis. **b** The correlation matrix reveals similarities between samples, indicating the high discriminatory power of the analyzed genes. **c** Markers of the undifferentiated state, **d** endoderm markers, **e** ectoderm markers, and **f** mesoderm markers display distinct gene expression patterns between differentiation states. **c–f** Mean \pm standard deviation of a total of $n = 105$ independent samples

split by differentiation state and protocol are annotated within the graphs. **g** Machine learning-based models can be used to identify differentiation states by analyzing qPCR-based gene expression data. The graph shows the results of $n = 10$ resamples of each of the displayed models. Median \pm standard deviation are annotated within the graphs. ΔC_t ; normalized (to *ACTB* and *GAPDH*) gene expression of analyzed samples. In (a), the qPCR device icon was created with BioRender.com released under a Creative Commons Attribution-NonCommercial-NoDerivs 4.0 International license.

mirrors diverse experimental conditions encountered in practical applications and enhances the utility of the hiPSCORE in various research settings. We differentiated three different iPSC lines into hepatocyte-like cells (HLCs, endoderm), hematopoietic progenitor cells (HPCs, mesoderm), and midbrain neurons (ectoderm) to account for further lineage commitment (Fig. 6a).

We sampled total RNA at the intermediate primary germ layer steps and performed the respective hiPSCORE subtests for endoderm, mesoderm, and ectoderm following lineage specification. In all cases except one, where the total RNA amount was insufficient for qPCR analysis, the hiPSCORE germ layer-specific tests were passed successfully. Subsequently, cells successfully differentiated into HLCs as

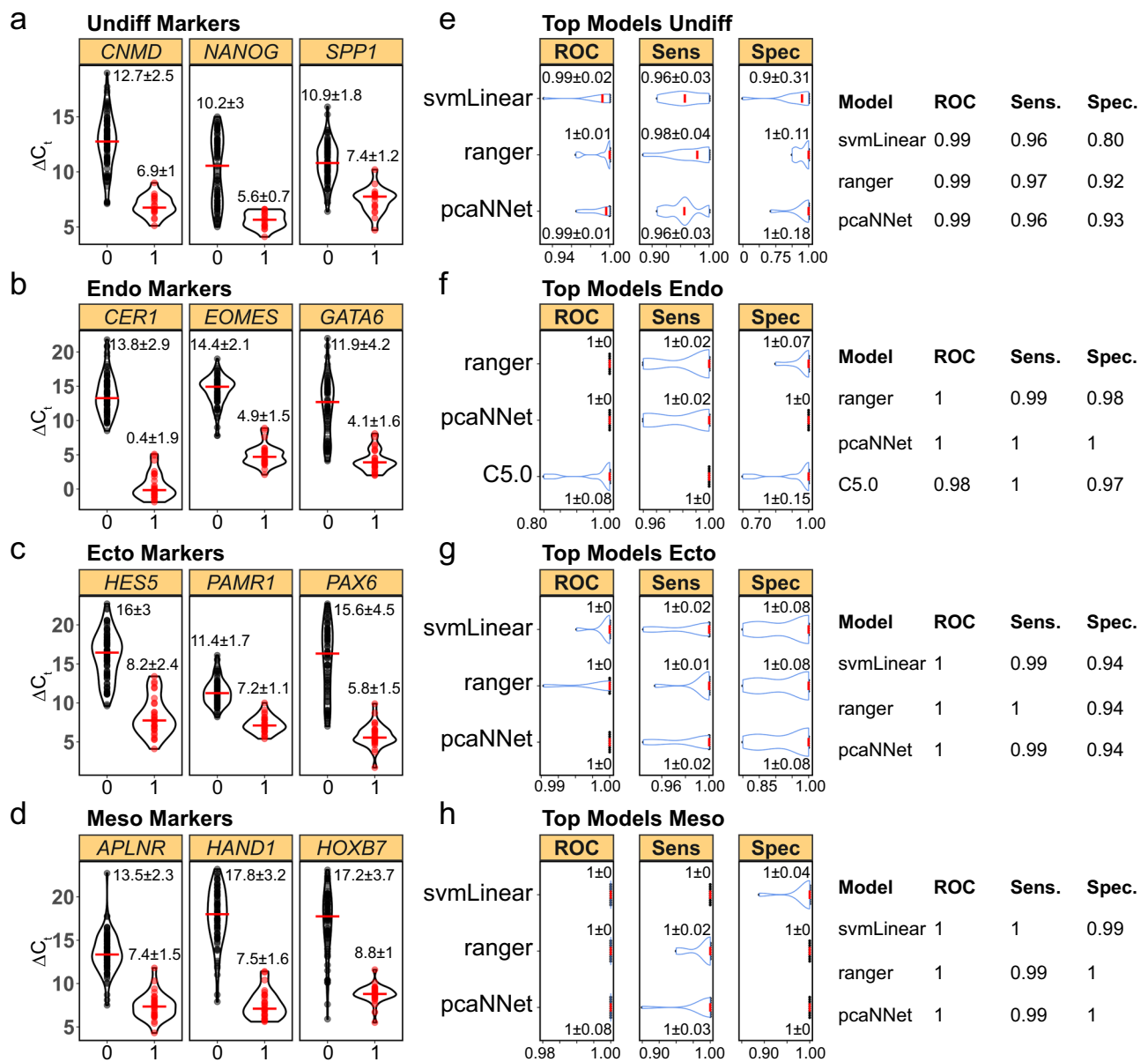


Fig. 4 | Predictive power of the tested models on human induced pluripotent stem cell differentiation states. A combination of three genes per differentiation state, i.e., **a** undifferentiated human induced pluripotent stem cells (iPSCs), **b** endoderm, **c** ectoderm, and **d** mesoderm, was used to train models to classify samples. **a–d** Mean ± standard deviation of a total of $n = 105$ independent samples split by binary dummy-coded classification state are annotated within the graphs. Highly accurate models for **(e)** undifferentiated iPSCs, **f** endoderm-, **g** ectoderm-,

and **h** mesoderm-differentiated iPSCs were identified which are able to discriminate individual samples with high power, sensitivity, and specificity. **e–h** Graphs show the results of $n = 10$ resamples of each of the displayed models. Median ± standard deviation are annotated within the graphs. The quality metrics of the final models are reported in the tables next to each graph. ΔC_t : normalized (to *ACTB* and *GAPDH*) gene expression of analyzed samples. ROC receiver operating characteristic, Sens sensitivity, Spec specificity.

indicated by upregulation of *ALB*, *TF*, and *TTR* (Fig. 6b), into HPCs as indicated by upregulation of surface markers CD43, CD34, and CD45 (Fig. 6c), and into midbrain neurons as indicated by neuronal morphology and characteristic β 3-tubulin and tyrosine hydroxylase staining (Fig. 6d).

Next, we extended the experimental validation of further lineage specification to more complex 3D organoid structures following differentiation into each of the three primary germ layers. For an endoderm-derived organoid, we differentiated iPSCs into branching lung organoids (BLOs, Fig. 7a and Supplementary Fig. 11a). After confirming successful endoderm differentiation by the hiPSCore mesoderm substest, flow cytometry, and gene expression analysis (Supplementary Fig. 11b), BLOs were differentiated and matured for up to 86 days. The presence of specialized cell types as determined by IF

staining and gene expression analysis (Supplementary Fig. 11c) indicated successful maturation into BLOs.

For a mesoderm-derived organoid, we differentiated iPSCs into blood vessel organoids (BVOs, Fig. 7b and Supplementary Fig. 12a). After confirming successful mesoderm differentiation by the hiPSCore mesoderm substest, BVOs were successfully generated as indicated by characteristic IF staining of endothelial-specific markers CD31 and VE-CAD (Supplementary Fig. 12b).

Finally, we generated cortical brain organoids³⁶ (BOs, Fig. 7c and Supplementary Fig. 13a). After confirming successful ectoderm differentiation by employing the hiPSCore ectoderm substest, we matured BOs for up to 80 days and observed brain region-specific patterning as indicated by *TBR1/PAX6* (Supplementary Fig. 13b), *SOX2/SATB2* (Supplementary Fig. 13c), *TBR2/PAX6* (Supplementary Fig. 13d), and

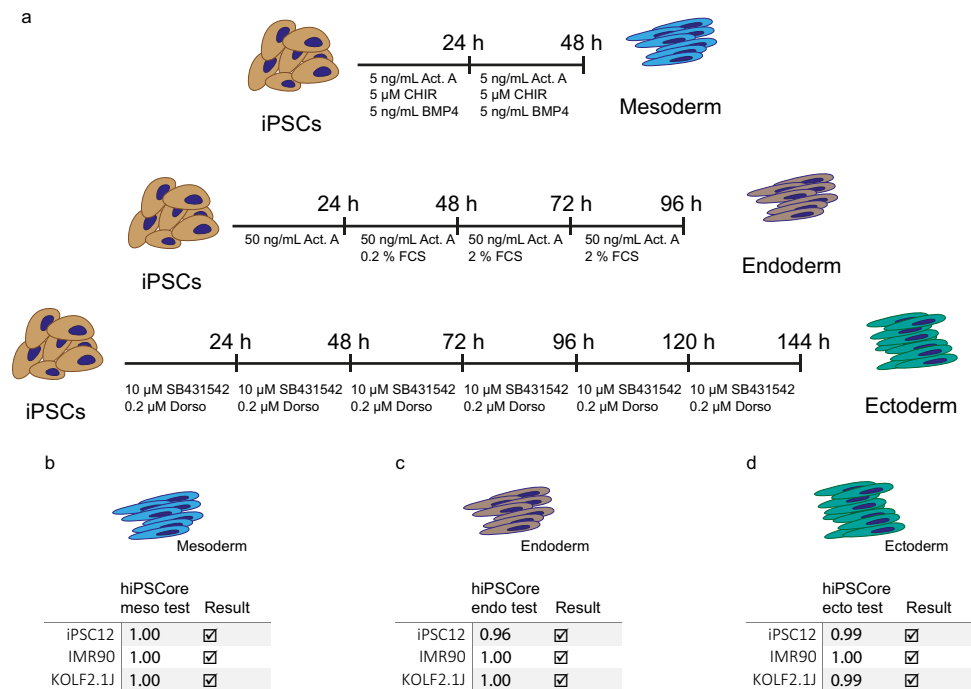


Fig. 5 | The hiPSCore classification can be applied to custom protocols for directed trilineage differentiation of human induced pluripotent stem cells.
a Three different human induced pluripotent stem cell (iPSC) lines were differentiated into mesoderm, endoderm, and ectoderm using growth factors and small

molecules. Afterwards, they were analyzed with the hiPSCore classification algorithm, revealing successful differentiation into **b** mesoderm, **c** endoderm, and **d** ectoderm. These results support the applicability of the hiPSCore classification for a broader range of directed differentiation protocols.

β 3-tubulin/FOXP1 (Supplementary Fig. 13e) IF staining. Taken together, these results underscore the importance of the validated hiPSCore gene set. This, combined with the hiPSCore machine learning-based classification, enables assessing the potential of iPSCs for successful differentiation into precursor cells, thereby signaling their ability to advance toward more specialized lineages.

Discussion

iPSC validation and quality control procedures are crucial for ensuring consistent and meaningful outcomes in scientific and translational applications^{5,12,17,18,37}. Consequently, it is paramount to assess their bona fide identity, genome integrity, and differentiation capacity. Hence, addressing the challenges presented by laborious and non-standardized testing methods, along with the absence of uniquely discriminating cell fate markers, is imperative. Consequently, a re-evaluation of marker genes to assess the differentiation states of iPSC lines became necessary.

Based on extensively cross-validated data derived from 15 different undifferentiated and differentiated iPSC lines, we observed the lack of predictive power to unequivocally identify differentiation states using currently recommended markers. We leveraged this robust dataset as a ground truth to identify and validate a set of 14 genes (three per germ layer and the undifferentiated state plus two reference genes). These genes exhibit high discriminatory power for early germ layer differentiation states. This was demonstrated by integrating the collected data into a machine learning-driven classification model we named hiPSCore. In particular, the hiPSCore classification approach is a supervised machine learning binary classification model based on dummy-coded variables. In total, we used 25 iPSC lines with corresponding flow cytometry characterization to thoroughly validate our hiPSCore classification approach. Integrating four distinct classification models, one for each germ layer and the undifferentiated state, the hiPSCore approach emerges as a potent pluripotency test for directed trilineage differentiation. By demonstrating its applicability to custom protocols, our classification system allows for flexible, cost-

saving, tailored experimental design. Our findings illustrate the utility of the hiPSCore approach in predicting an iPSC line's likelihood of progressing beyond primary germ layer specification, as evidenced by subsequent lineage specification and maturation into intricate 3D organoid structures. The versatility of our classification system extends to diverse culture systems, reflecting the range of experimental conditions encountered in practical applications. This broad applicability enhances its utility across various research settings.

While a variety of tools exist to assess pluripotency, they all come with major drawbacks. Predicting the pluripotent potential of iPSCs by analyzing pluripotency signatures by microarray/transcriptome sequencing³⁸ is limited in many labs due to the high cost of the instruments or high per sample cost when outsourcing this as a service. Furthermore, functional pluripotency through germ layer differentiation evaluation is not assessed. The same holds true for methods based on the analysis of epigenetic signatures by bisulfite conversion and pyrosequencing, with the addition of low multiplexing capacity³⁹. The latter may also be used to assess functional pluripotency but exhibits the same drawbacks⁴⁰. Functional pluripotency of trilineage-differentiated iPSCs can also be assessed by antibodies, as we also used for cross-validation in this study. Compared to qPCR, antibody-based analysis comes with increased hands-on time, cost, and decreased multiplexing capacity. Currently available qPCR-based solutions to assess functional differentiation are tailored to EB-based spontaneous differentiation and make use of a high number of marker genes, making multiplexing rather expensive^{24,25}.

Moreover, the lack of established thresholds impedes the standardization of pluripotency testing. Further studies can enhance or refine this standardization, building upon our identified gene panel to validate, expand or reduce, and contextualize listed markers. Elucidation of their surrogate or essential roles during differentiation will also be the subject of future studies.

Our study has three major implications for the stem cell field. (1) We extensively validated a set of marker genes, some of which have not previously been used in the context of iPSC pluripotency testing. This

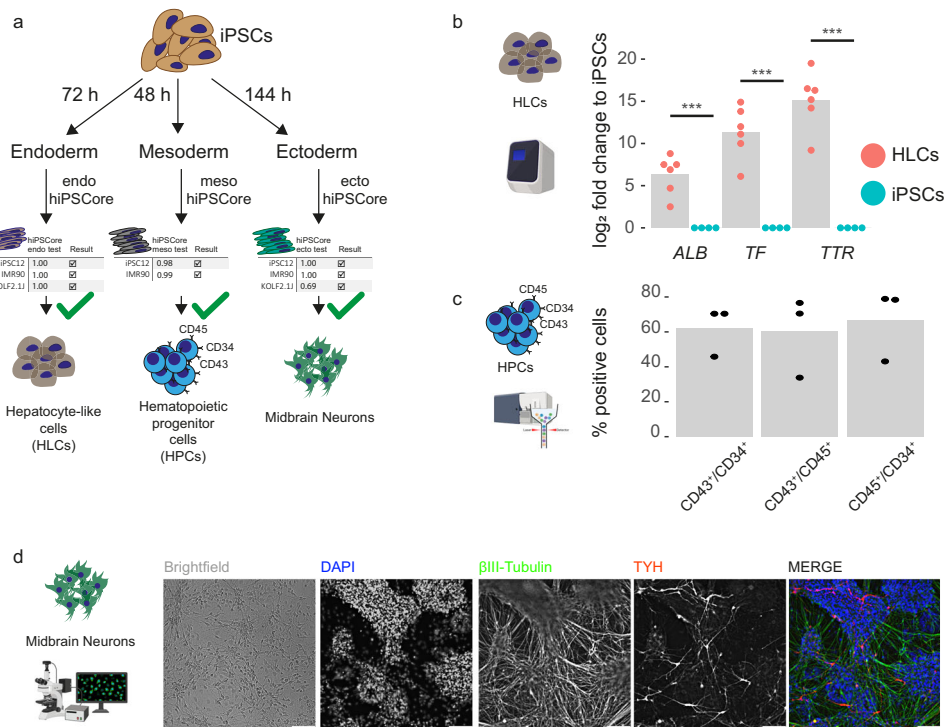


Fig. 6 | Human induced pluripotent stem cells differentiate into specialized cell types for each primary germ layer. a Three different human induced pluripotent stem cell (iPSC) lines were differentiated into endoderm, mesoderm, and ectoderm primary germ layer cells before continuing lineage specification into hepatocyte-like cells (HLCs), hematopoietic progenitor cells (HPCs), and midbrain neurons. **b** To verify successful hepatic lineage specification, gene expression levels of HLCs were analyzed for upregulation of hepatocyte-specific markers *ALB*, *TF*, and *TTR* (normalized to *ACTB* and *GAPDH*). Relative gene expression levels were determined by the $\Delta\Delta C_t$ method relative to the respective undifferentiated iPSCs. Statistical testing was performed using individual Welch's two sample two-sided *t*-tests and significance was inferred at $p \leq 0.05$. *** $p \leq 0.001$; exact *p* values to the first non-

zero digit are as follows: *ALB*: 0.001, *TF*: 0.0002, *TTR*: 0.0001. **c** To verify successful hematopoietic lineage specification, surface levels of hematopoiesis-specific CD43, CD34, and CD45 were determined by flow cytometry. Double-positive CD43/CD34, CD43/CD45, and CD45/CD34 populations of HPCs derived from $n = 3$ independent iPSC lines are shown. **d** To verify successful neural lineage specification, midbrain neurons were stained for neuronal markers β 3-tubulin and tyrosine hydroxylase (TYH), indicating successful midbrain neuron differentiation. Example images are shown for $n = 3$ independent cell lines. Scale bar: 100 μ m. The qPCR device icon (in **b**), the flow cytometry device icon (in **c**), and the fluorescent microscopy icon (in **d**) were created with BioRender.com released under a Creative Commons Attribution-NonCommercial-NoDerivs 4.0 International license.

list holds the potential for refining the current guidelines. In fact, only four out of the selected final set of 12 genes were recommended (as of the 2023 ISSCR guidelines) as markers of at least one of the four differentiation states investigated in this study. Only one of these genes is listed as a unique marker (*NANOG* for the undifferentiated state), whereas the remaining three are each listed for two differentiation states simultaneously (*PAX6* for endoderm and ectoderm; *GATA6* for endoderm and the undifferentiated state; *HAND1* for endoderm and mesoderm). This underlines the importance of careful validation of marker genes used in qPCR. (2) We developed a streamlined, standardized, easy-to-follow, and cost-effective pipeline for stem cell identity assessment. This approach enables the broad use of iPSCs with appropriate early quality control, which is especially important considering the already large and rising number of laboratories working with iPSCs. (3) We developed and established a machine learning-based classification approach, the hiPSCore classification score. This score serves as a tool to standardize early iPSC quality control.

To enable immediate implementation of our findings, we have developed a user-friendly web application based on R Shiny (see "Methods" section). This tool incorporates the machine learning models described in this manuscript, making our research directly applicable to laboratory workflows.

To date, there is no existing assay specifically tailored to directed trilineage differentiation, utilizing the optimal number of marker genes per germ layer. The development of such an assay represents a substantial leap forward in enhancing iPSC quality control and promoting comparability across diverse institutions. The database used to

develop our models will grow over time, enhancing the robustness of their predictive power and enabling reliable multi-class classification of increasingly complex samples. To ensure the accuracy and replicability of cell fate identification, it is imperative to validate core markers through rigorous testing. Since it is impractical that each laboratory develops its own extensive validation and classification protocols, standardization is essential. We envision extending our scoring approach by incorporating advanced capabilities to refine our machine-learning models. This will include evaluating additional iPSC-derived cell types, such as neurons and endothelial cells, as well as human embryonic stem cells and naive pluripotent stem cells, for more precise and comprehensive assessments. In this way, scientific progress can be made as a collaborative effort, and the development of standards can be more streamlined. In conclusion, our findings provide a substantial advancement to accurately characterize undifferentiated and differentiated states of iPSCs. This work not only refines our understanding of iPSC quality control but also paves the way for more robust and reliable applications in both research and regenerative medicine.

Methods

Cell culture

Human iPSCs cells were purchased from different vendors, reprogrammed in-house, obtained by material transfer agreement, or genome-edited in-house, respectively (see Supplementary Table 1 for details of all iPSC lines employed in this study). iPSCs were grown in mTeSR Plus (STEMCELL Technologies) complete medium on 6-well

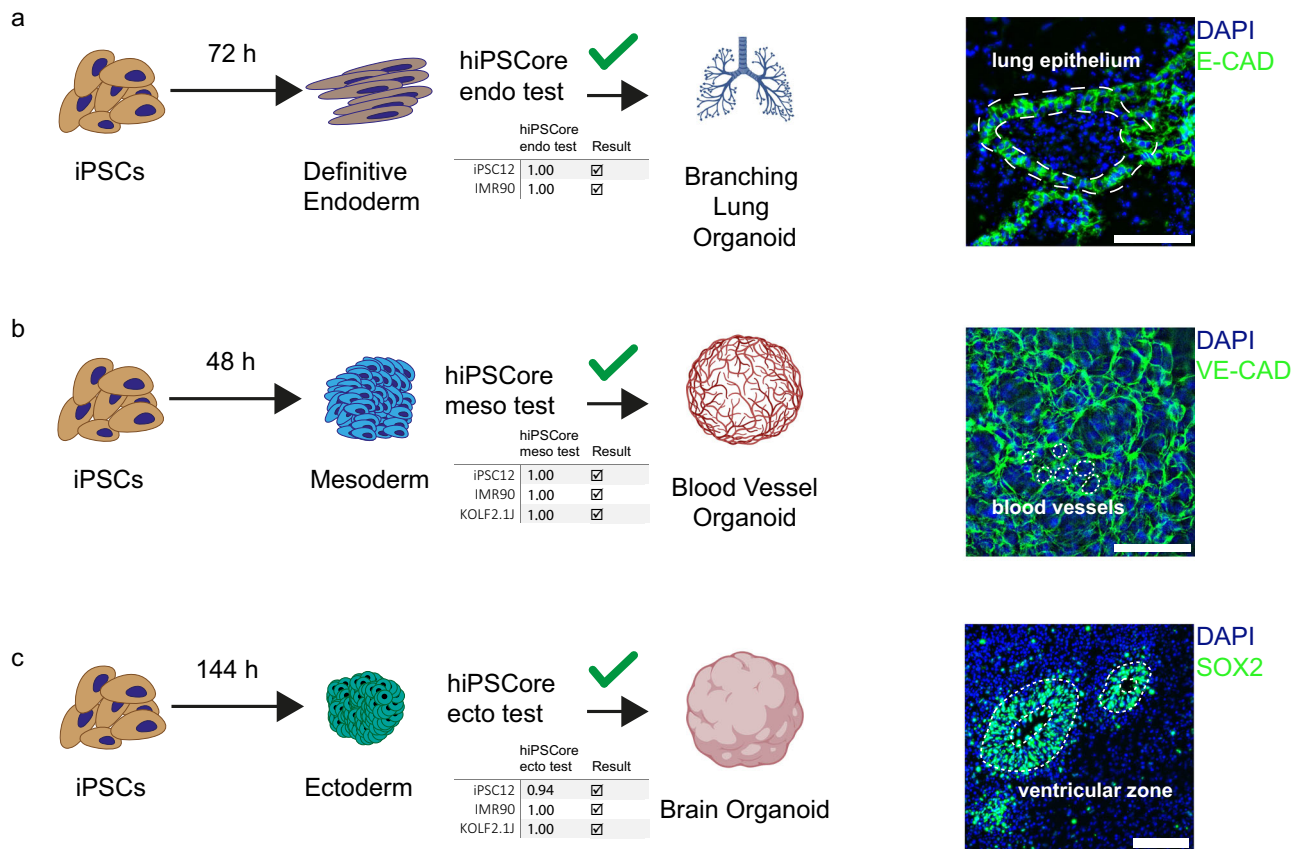


Fig. 7 | Human induced pluripotent stem cells differentiate into complex 3D organoids. a The hiPSCore endoderm substest can be used to assess definitive endoderm differentiation to assess whether human induced pluripotent stem cells (iPSCs) can differentiate into branching lung organoids. The resulting branching lung organoids consist of specialized cell types. Dashed white lines mark lung epithelium as indicated by epithelial E-CAD staining. The shown image is processed from a staining shown in Supplementary Fig. 11. **b** The hiPSCore mesoderm substest can be used to assess mesoderm differentiation to assess whether human iPSCs can differentiate into blood vessels. The resulting blood vessel organoids consist of endothelial cells. Dashed white lines mark blood vessels as indicated by endothelial VE-CAD staining. The shown image is a zoom-in of a staining shown in

Supplementary Fig. 12. **c** The hiPSCore ectoderm substest can be used to assess neuroectoderm differentiation to assess whether human iPSCs can differentiate into cortical brain organoids. The resulting brain organoids consist of specialized cell types. Dashed white lines mark ventricular zones as indicated by patterned SOX2 staining. The shown image is processed from a staining shown in Supplementary Fig. 13. Immunofluorescent images are representative of $n = 3$ independent experiments using at least two different independent iPSC lines. Scale bars: 100 μm . The branching lung organoid icon (in **a**), the blood vessel organoid icon (in **b**), and the brain organoid icon (in **c**) were created with BioRender.com released under a Creative Commons Attribution-NonCommercial-NoDerivs 4.0 International license.

plates coated with growth factor-reduced Geltrex (Thermo Fisher). All cell lines were routinely tested for mycoplasma contamination using either a PCR (Minerva Biolabs) or an enzyme-based (Vazyme) test. At the start of the study, all cell lines were karyotypically normal, as assessed by G-banding and were authenticated through short tandem repeat profiling.

Genome engineering

Genome engineering of iPSC lines was performed as previously described⁴¹. Guide RNAs for *KCNK2* (5'→3': CTTGGTTTCTC TTGGC) and *AHR* (5'→3': AAGTCGGTCTCTATGCCGCT) were used to generate gene knockouts. Following cell expansion, single cell-seeded clones were lysed in proteinase K (0.2 mg/mL), and their genotypes were determined through deep sequencing using a MiSeq benchtop sequencer (Illumina) using a nano V2 cassette and targeting ~2000 reads/clone (San Diego, CA). Data were acquired in FASTQ format and analyzed using OutKnocker⁴².

Directed trilineage differentiation

Directed differentiation of human iPSCs into the three primary germ layers was performed by employing two different commercially available kits: the StemMACS Trilineage Differentiation Kit (Miltenyi

Biotech) and the STEMdiff Trilineage Differentiation Kit (STEMCELL Technologies) according to the manufacturers' instructions with minor adjustments. In brief, 5×10^4 (mesoderm) or 2×10^5 (endoderm, ectoderm) iPSCs were seeded for differentiation into Geltrex-coated wells of a 24-well plate. Differentiation media volumes were reduced to 500 μl /media change (750 μl for Mesoderm-I of the StemMACS Trilineage Differentiation Kit) to increase sample throughput. After 5 (STEMdiff: endoderm, mesoderm) and 7 days (for STEMdiff: ectoderm; StemMACS: all germ layers) of differentiation, cells were washed twice with PBS and lysed with 300 μl Trizol (Thermo Fisher) or subjected to flow cytometry analysis. For directed trilineage differentiation employing custom protocols, 5×10^4 (mesoderm) or 2×10^5 (endoderm, ectoderm) cells were seeded into Geltrex-coated wells of a 24-well plate. For mesoderm differentiation, a modified version of a protocol described by Zhang et al. was followed⁴³. RPMI1640 base medium was supplemented with 5 ng/mL Activin A (STEMCELL Technologies), 5 μM CHIR99021 (Peprtech), and 5 ng/mL BMP4 (Peprtech). Growth factors were added fresh to the base medium, and the differentiation medium was changed once after 24 h. After a total of 48 h, mesodermal cells were harvested and lysed with Trizol. For endoderm differentiation, a protocol described by Tiwari et al. was followed⁴⁴. RPMI1640 base medium was supplemented with 50 ng/mL

Activin A, and cells were incubated for 24 h, followed by incubation with RPMI640 supplemented with 50 ng/mL Activin A and 0.2% FCS (Gibco) for another 24 h. Two additional medium changes each after 24 h were performed with RPMI640 base medium supplemented with 50 ng/mL Activin A and 2% FCS for a total of 96 h of differentiation, after which endodermal cells were harvested and lysed with Trizol. For ectoderm differentiation, dual SMAD inhibition (SMADi) based on a modified protocol described by Lu et al. was performed⁴⁵. Essential-6 (E6, Thermo Fisher) medium was supplemented with 0.2 μ M Dorsomorphin (Selleckchem) and 10 μ M SB-431542 (Selleckchem). SMADi medium was changed every 24 h with freshly added Dorsomorphin and SB-431542. After a total of 144 h of incubation, cells were harvested with Accutase (PanBiotech) and lysed with Trizol.

Flow cytometry analysis of directed trilineage differentiation

Human iPSCs were differentiated into the three primary germ layers endoderm, mesoderm, and ectoderm, according to the protocol described above. Alternatively, the undifferentiated state was maintained. On the final day (either 5 or 7, see above), cells were harvested as single cells with Accutase into FACS buffer (2% FBS in PBS), counted, fixed with 4% PFA for 15 min, washed with FACS buffer, and distributed into 1.5 mL reaction tubes at a concentration of $1-3 \times 10^5$ cells per staining condition. Antibodies for surface marker proteins (undifferentiated: SSEA-4; endoderm: CXCR4; mesoderm: CD140b) were added, diluted in 50 μ l FACS buffer and incubated for 30 min in the dark. For staining of intracellular marker proteins, cells were washed with FACS buffer and permeabilized with 0.5 mL Saponin buffer (1 mg/mL Saponin in 1% BSA in PBS) for 15 min in the dark. Afterwards, samples were incubated with appropriate antibodies (undifferentiated: Oct3/4; endoderm: SOX17; ectoderm: PAX6, SOX2; mesoderm: T/BRACHYURY) diluted in 50 μ l Saponin buffer for 30 min in the dark. All primary antibodies, except T/BRACHYURY (R&D), were purchased from Miltenyi Biotec. Samples were washed with 0.5 mL Saponin buffer and T/BRACHYURY-stained mesoderm samples were incubated with appropriate fluorescently labeled secondary antibodies (Thermo Fisher; Jackson) diluted in 50 μ l Saponin buffer for 20 min in the dark. Finally, samples were resuspended in FACS buffer and analyzed on a FACS Canto II (Becton Dickinson). Analysis and visualization (Supplementary Fig. 14a) were performed using FlowJo v10.10.0 (Becton Dickinson) and the statistical programming language R. All antibodies used and their corresponding dilutions are reported in Supplementary Table 5.

Hepatocyte-like cell differentiation

Human iPSCs (iPSC12, IMR90, KOLF2.1J) were differentiated into the endodermal lineage by employing the first steps of the STEMdiff Branching Lung Organoid Kit (STEMCELL Technologies) according to the manufacturer's instructions until the definitive endoderm stage. Alternatively, cells were differentiated into the endodermal lineage by employing the STEMdiff Trilineage Differentiation Kit as described above. After endoderm induction, replicates were harvested and subjected to the hiPSCore endoderm test (as described in the "Methods" section for hiPSCore). Afterwards, endodermal cells were differentiated into HLCs following a protocol described by Graffman et al.⁴⁶. Hepatocyte differentiation media (Knockout DMEM (Thermo Fisher) containing 20% Knockout Serum Replacement (Thermo Fisher) and 1% penicillin/streptomycin (PanBiotech)) was changed daily. After a total of 12–19 days, cells were harvested using Accutase and lysed with Trizol. Total RNA was extracted, reverse transcribed into cDNA, and the gene expression levels of hepatocyte-specific genes (*ALB*, *TF*, and *TTR*) were analyzed by qPCR using the $\Delta\Delta C_t$ method normalized to *GAPDH* and *ACTB* relative to the respective undifferentiated iPSC lines. All primer sequences used are reported in Supplementary Table 6.

Hematopoietic progenitor cell differentiation

Human iPSCs (iPSC12, IMR90, KOLF2.1J) were differentiated into HPCs using the STEMdiff Hematopoietic Kit (STEMCELL Technologies) according to the manufacturer's instructions. After mesoderm induction, cells were harvested with Accutase, lysed with Trizol, and total RNA extracted. Afterwards, the hiPSCore mesoderm test was performed and replicates were subjected to HPC differentiation. Success of HPC differentiation was determined by flow cytometry using antibodies for the surface marker proteins CD34, CD43, and CD45 (STEMCELL Technologies) diluted in cold FACS buffer. To discriminate between live and dead cells, DAPI (Sigma) was added directly before the analysis on a FACS Canto II flow cytometer. The gating strategy is visualized in Supplementary Fig. 14b. In general, total RNA yield can be very low because the protocol requires very scarce seeding densities (for the KOLF2.1J line, we did not obtain enough RNA to perform the test). It has to be noted that, although it is possible, it is likely not feasible to check for successful mesoderm differentiation within the context of this protocol due to the high cost to obtain enough RNA to generate cDNA and perform qPCR. All antibodies used and their corresponding dilutions are reported in Supplementary Table 5.

Midbrain neurons differentiation

Human iPSCs (iPSC12, IMR90, KOLF2.1J) were differentiated into midbrain dopaminergic neurons using the STEMdiff SMADi Neural Induction Kit (STEMCELL Technologies), the STEMdiff Midbrain Neuron Differentiation Kit (STEMCELL Technologies), and the STEMdiff Midbrain Neuron Maturation Kit (STEMCELL Technologies) according to the manufacturer's instructions. Plates were coated with either Geltrex or Poly-L-Ornithin (Sigma)/Laminin (BioLamina) to obtain two technical replicates of each parental iPSC line. Success of ectoderm induction was determined by analyzing RNA at day 6 of the differentiation using the hiPSCore ectoderm test. After 18 days of midbrain maturation (41 days after the start of ectoderm induction), cells were washed twice with PBS containing calcium and magnesium (Gibco), fixed for 15 min at RT, washed twice with PBS containing calcium and magnesium, permeabilized with 0.1% Triton X-100 (Carl Roth) for 1 h at RT, washed once with PBS containing calcium and magnesium, blocked with 3% BSA in PBS for 2 h at RT, and incubated overnight at 4 °C with antibodies for β -tubulin (Sigma) and tyrosine hydroxylase (Merck Millipore) diluted in 3% BSA in PBS. Afterwards, cells were washed three times with PBS containing calcium and magnesium, and primary antibody binding was visualized using appropriate fluorescent secondary antibodies (Dianova, Thermo Fisher) after incubation for 1 h at RT. Cells were washed three times with PBS containing calcium and magnesium and in the last step DAPI was added at 100 ng/mL for counterstaining of nuclei. Finally, stained midbrain dopaminergic neurons were imaged using the THUNDER Imager 3D Live Cell & Cell Culture microscope (Leica). All antibodies used and their corresponding dilutions are reported in Supplementary Table 5.

Branching lung organoid differentiation

Human iPSCs (iPSC12, IMR90) were differentiated into BLOs using the STEMdiff Branching Lung Organoid Kit (STEMCELL Technologies) according to the manufacturer's instructions. After the definitive endoderm step, cells were harvested for analysis. The success of endodermal lineage specification was assessed with flow cytometry using an antibody for the surface protein marker CXCR4 (R&D) and an appropriate Alexa Fluor 647-conjugated secondary antibody according to the protocol described above for surface staining. Definitive endoderm specification was also assessed with the hiPSCore endoderm test. Afterwards, cells were differentiated into anterior foregut endoderm, and free-floating anterior foregut endoderm spheroids were embedded into a Geltrex sandwich on 24-well transwell inserts. BLOs were maintained for up to 86 days before they were harvested into Trizol or fixed, frozen in O.C.T. Compound (TissueTek),

cryosectioned and stained with H&E, or permeabilized with ice-cold methanol and acetone, each for 10 min, and stained with antibodies for E-CAD (Cell Signaling Technologies), acetylated tubulin (Sigma), VIM (Cell Signaling Technologies), TTF1 (Thermo Fisher), AQP5 (Alomone), and pan-cytoKRT (Thermo Fisher), followed by appropriate secondary antibody staining, to detect specialized cell types. Hoechst 33342 (Thermo Fisher) was used to counterstain nuclei. All antibodies used and their corresponding dilutions are reported in Supplementary Table 5.

Blood vessel organoid differentiation

Human iPSCs (iPSC12, IMR90, KOLF2.1J) were differentiated into BVOs using the STEMdiff Blood Vessel Organoid Kit (STEMCELL Technologies) according to the manufacturer's instructions. After mesoderm induction, half of the mesodermal spheroids were harvested into Trizol and analyzed using the hiPSCore mesoderm test. The rest of the cells was further differentiated into vascular networks and BVOs. After 21 days of differentiation, BVOs were washed twice with PBS, fixed with 4% PFA in PBS for 20 min rocking at RT, washed two times with PBS, blocked for 3 h rocking at RT with blocking buffer (1% BSA, 3% FBS, 0.5% Tween 20, 0.5% Triton X-100, 0.01% sodium deoxycholate solution (1% wt/vol) in PBS), and incubated with primary antibodies for CD31/PECAM-1 (Santa Cruz) and VE-CAD/CD144 (Thermo Fisher) overnight shaking at 400 rpm covered with aluminum foil in a thermoblock set to 4 °C. Afterwards, BVOs were washed three times with wash buffer (0.05% Tween 20 in PBS) on a rocking platform at RT, incubated with fluorescently conjugated secondary antibody (Dianova) in blocking buffer for 3 h on a rocking platform at RT in the dark, and washed three times with wash buffer for 30 min on a rocking platform at RT in the dark. For counterstaining, BVOs were incubated with DAPI at 1 µg/mL for 10 min on a rocking platform at RT in the dark. Afterwards, BVOs were washed for 10 min on a rocking platform at RT with PBS in the dark. For clearing, individual BVOs were transferred to a 48-well cell culture plate containing RapiClear 1.47 (SUNJin Lab) pre-warmed to RT and incubated for 16 h on a rocking platform in the dark. Cleared BVOs were embedded in RapiClear 1.47 and imaged using the THUNDER Imager 3D Live Cell & Cell Culture microscope.

Cortical brain organoid differentiation

Human iPSCs (iPSC12, IMR90, KOLF2.1J) were differentiated into cortical BOs (dorsal forebrain) based on a modified version of the protocol described by Sloan et al.³⁶. For EB formation, 1×10^3 cells were seeded into Biofloat Flex (FaCellitate) coating solution-coated U-shaped round-bottom wells of a 96-well plate containing 100 µl mTeSR Plus and 10 µM Y-27632 dihydrochloride (Absource). After 24 h (day -1), 50 µl of the seeding medium was removed and 100 µl of E6 medium containing 1% penicillin/streptomycin containing 10 µM Y-27632 dihydrochloride was added on top. After 24 h (day 0), differentiation of the EBs into neuroectoderm was initiated using SMADi by replacing 100 µl of the medium with SMADi medium (E6 containing 1% penicillin/streptomycin and freshly added 5 µM Dorsomorphine and 10 µM SB-431542). This medium change was performed daily until day 3 with 10 µM Y-27632 dihydrochloride and from then daily until day 6 without additional Y-27632 dihydrochloride. On day 6, up to eight aggregates/well were transferred to a 6-well plate containing Neurobasal A (Thermo Fisher) medium and washed two times with Neurobasal A medium before NDM medium (Neurobasal A, 2% B27 supplement (Capricorn Scientific), 1% penicillin/streptomycin, and 1% GlutaMAX) with freshly added 20 ng/mL EGF (Peprotech) and 20 ng/mL FGF (Peprotech) was added to the cells. Aggregates were incubated by shaking at 60 rpm at 37 °C, and NDM medium containing EGF and FGF was changed daily until day 16, upon which medium change was performed every 2 days until day 25. From day 25 on, NDM medium was freshly supplemented with 20 ng/mL BDNF and 20 ng/mL NT-3 and changed every two days. From day 43, medium change was reduced to

every 3–4 days, and NDM medium without additional factors was used. BOs were maintained for up to 80 days, collected, washed with PBS, and fixed in 4% PFA in PBS for 1 h. For cryopreservation, BOs were incubated in 30% sucrose at 4 °C overnight and afterwards embedded with O.C.T. Compound in square molds and snap-frozen on dry ice. The embedded BOs were stored at -80 °C until 10 µm thin sections were cut with a cryostat (Leica) and collected on Superfrost Plus slides (Thermo Fisher). Sections were encircled with a hydrophobic PAP pen, washed with PBS to remove O.C.T. Compound, and stained with H&E or permeabilized with 0.5% Triton-X in PBS for antibody staining. For blocking, the sections were incubated with 3% BSA for 1 h at RT. Primary antibody incubation with TBR1 (Abcam), PAX6 (Santa Cruz), SOX2 (Cell Signaling Technologies), SATB2 (Santa Cruz), and TBR2 (Cell Signaling Technologies) was performed in 3% BSA for 2 h at RT in a humidified chamber. After washing with 3% BSA, the slides were incubated for 1 h with appropriate secondary antibodies and mounted in Fluoromount-G plus DAPI (Sigma). Stainings were visualized with a THUNDER Imager 3D Live Cell & Cell Culture microscope. All antibodies used and their corresponding dilutions are reported in Supplementary Table 5.

RNA isolation, cDNA transcription, and qPCR

Total RNA isolation was performed using the Direct-zol RNA Miniprep Kit (Zymo), including on-column DNase I digestion according to the manufacturer's instructions. RNA was eluted in 25 µl aqua dest., and the concentration was measured on a NanoDrop 2000 spectrophotometer (Thermo Fisher). One microgram of total RNA was reverse transcribed using the HiScript III RT SuperMix for qPCR kit (Vazyme). Afterwards, cDNA was diluted 1/10 with aqua dest. and used in a 10 µl qPCR reaction consisting of 5 µl ChamQ Universal SYBR qPCR Master Mix (Vazyme), 3 µl aqua dest., 1 µl primer mix (forward + reverse at 2.5 µM each for a final primer concentration of 250 nM), and 1 µl diluted cDNA sample. Reactions were run on a QuantStudio 3 (Thermo Fisher) qPCR cycler with a fast qPCR program (3 s denaturation, 20 s annealing and extension) for 40 cycles, followed by a melting curve analysis. Gene expression was normalized to the mean of two reference genes, *ACTB* and *GAPDH* ($\Delta\Delta C_t$). For primer sequences, see Supplementary Table 6.

Oxford Nanopore Technologies long-read transcriptome sequencing

Two hundred nanograms of total RNA of two biological replicates of undifferentiated iPSCs and respective differentiated cells generated with the StemMACS Trilineage Differentiation Kit (Miltenyi Biotec) were used for first strand cDNA synthesis in a 6 µl reaction consisting of 2 µl 10 µM RT primer (5'→3': AAG CAG TGG TAT CAA CGC AGA GTA CTT TTT TTT TTT TTT TTT TTT TTT TTT TV), 1 µl dNTPs (10 mM each, Vazyme) and aqua dest. up to 6 µl for 5 min at 70 °C. Second strand synthesis was performed by adding 2.5 µl Template Switching Buffer (New England Biolabs), 0.5 µl 75 µM Template Switching Oligo (5'→3': GCT AAT CAT TGC AAG CAG TGG TAT CAA CGC AGA GTA CAT rGrGrG) and 1 µl Template Switching RT Enzyme Mix (New England Biolabs) to the first strand reaction and incubating for 90 min at 42 °C, followed by heat inactivation at 85 °C for 5 min. Afterwards, 10 µl double-stranded cDNA (ds-cDNA) was amplified by adding 25 µl Phanta Max Buffer (Vazyme), 1 µl dNTPs (10 mM each, Vazyme), 2 µl Phanta Max Super Fidelity Polymerase (Vazyme), 1 µl 10 µM cDNA PCR Primer (5'→3': AAG CAG TGG TAT CAA CGC AGA GT), and 11 µl aqua dest. and performing a 7 cycles PCR reaction (45 s initial denaturation at 98 °C followed by 7 cycles 10 s at 98 °C, 15 s at 64 °C, 3 min at 72 °C, and a final elongation for 5 min at 72 °C). Afterwards, 1 µl of Exonuclease I (Thermo Fisher) was directly added to the PCR reaction and incubated for 15 min at 37 °C, followed by heat inactivation for 15 min at 80 °C. Final products were purified using AMPure XP (Beckham Coulter) beads at a ratio of 0.8 × PCR product to beads according to the manufacturer's instructions. ds-cDNA concentration was measured on a

Qubit Fluorometer (Thermo Fisher) using the dsDNA high sensitivity (HS) kit (Thermo Fisher).

Library preparation was performed according to the Ligation sequencing amplicons—Native Barcoding Kit 24 V14 (ONT, SQK-NBD114.24, protocol version NBA_9168_v114_revE_15Sep2022). Briefly, equal amounts of ds-cDNA (20.25 ng) were subjected to library preparation. The final library was quantified on a Qubit Fluorometer (Thermo Fisher) using the dsDNA HS kit (Thermo Fisher). Library size was determined using a D1000 ScreenTape assay (Agilent). A final library amount of 15 fmol was loaded on a PromethION Flow Cell (ONT) and sequenced on a P2 Solo (ONT) for 72 h.

For time series data analysis, cells were sampled at day 0 (undifferentiated), days 2 and 3 (endoderm, mesoderm), or at days 2, 3, and 5 (ectoderm) and processed for long-read transcriptome sequencing accordingly. In this case, the STEMCELL differentiation kit was used, as it uses the same media composition throughout the differentiation process, making data interpretation for intermediate states more feasible. The sequencing data parameters are reported in Supplementary Table 7.

Sequencing data analysis

Basecalling was performed using the guppy basecaller (v6.4.6) with a minimum quality threshold of 5. FASTQ files were concatenated and mapped to the reference genome (GRCh38) using Minimap2 (v2.24) with the options (-uf -k14) used for noisy direct RNA sequencing ONT reads to enhance sequence retrieval. All further analysis was performed using R (v4.2.2). Transcripts were counted using Rsubread (v2.12.3) featureCounts with options for long sequencing reads and GRCh38.106 to annotate transcripts. Low abundance transcripts were excluded by applying a threshold for the combined sum of counts of at least 23 over all eight samples. For shallow time series, the sum threshold was set to 6. Exploratory principal component analysis was performed using the R stats package (v4.3.2) based on raw sequencing counts.

Afterwards, reads were normalized to counts per million (cpm) using edgeR (v3.40.2, Supplementary Data 1). Significantly differential transcript abundance between germ layer differentiations and the undifferentiated state was assessed by using edgeR glmTreat with a “Benjamini–Hochberg” false discovery rate p value adjustment at a threshold of 0.05 (Supplementary Data 2). Transcripts with the potential to serve as markers were assessed by normalizing log₂ counts to the undifferentiated samples and filtering for high log₂ fold changes (l2fc, depending on the differentiation state, higher than 3–6 for differentiated samples and lower than –2 for each differentiated sample versus the undifferentiated pluripotent controls; Supplementary Data 3). Gene set enrichment analysis was performed using clusterProfiler (v4.10.1) with “Benjamini–Hochberg” post-hoc correction at a p value cutoff of 0.05. The mean of 10 repeats was calculated. For comparison of transcript detection of short- versus long-read sequencing data, we downloaded a total of 247 transcriptome sequencing datasets of undifferentiated iPSCs from the Human Induced Pluripotent Stem Cell Initiative (<https://www.hipsci.org/>, see Source Data file for complete list of samples), converted the length-normalized counts to cpm, and compared expression signatures to our long-read transcriptome sequencing data. All data were visualized using ggplot2 (v3.4.2) and ComplexHeatmap (v2.14).

Machine learning

The machine learning implementation to classify samples was performed using the statistical programming language R with the caret framework⁴⁷. ΔC_t -normalized (to *GAPDH* and *ACTB*) gene expression values were obtained from a total of 105 biological samples derived from 15 different human iPSC lines (undifferentiated: 15 samples; germ layers: 90 samples from 15 iPSC lines differentiated into each endoderm, ectoderm, and mesoderm by each of the two different

commercially available kits). These total of 1260 data points (12 genes/sample) were used as the ground truth to train a machine learning-based classification system. To that end, each data point was classified in a dummy-coded binary classification system as either “0” for a negative combination (e.g., an iPSC-derived endoderm, ectoderm, or mesoderm sample analyzed for *NANOG* expression) or “1” for a positive combination (e.g., an undifferentiated iPSC sample analyzed for *NANOG* expression). Afterwards, the dataset was split 70:30 into training and testing data and used to train different models, including random forests and neural networks. Three genes per germ layer were used to train the models. Model parameters were tuned using tenfold repeated cross-validation with three repeats. Afterwards, the best models for each germ layer were selected based on the ROC. All further classifications were performed on previously unseen data and cross-validated using further methods, e.g., lineage specification. For a comprehensive overview, see Supplementary Fig. 15a. For individual subtests, p values ≥ 0.75 are considered high confidence, p values ≥ 0.6 and < 0.75 are considered medium confidence, and lower p values < 0.6 are considered low confidence. A warning is issued if p values are < 0.75 for each differentiation state on average and/or if one or more of the individual subtests fail completely. The machine learning models have been implemented into the hiPSCore web-tool, which can be accessed at <http://jjobner.shinyapps.io/hipscore>. Currently, this tool accepts Excel results file outputs from QuantStudio 3 with samples denoted as “Control”, “Pluripotency”, “Endoderm”, “Ectoderm”, “Mesoderm”, and “a.dest”. Until further devices are implemented, users can use the input template file (available at <http://jjobner.shinyapps.io/hipscore>). After upload, users can obtain the hiPSCore in two different ways. (1) default: each differentiation state is evaluated based on the respective subtest, and the hiPSCore is calculated as a sum of the classification multiplied by the probability of the prediction p (Supplementary Fig. 15b). This implementation of the test asks, “Is this specific sample of this specific (undifferentiated/endoderm/ectoderm/mesoderm) cell fate identity?”, i.e., a binary classification (Yes/No). (2) germ layer: samples are classified based on the complete gene signature of all 12 target genes (plus 2 reference genes), and the classification is reported based on the class probability p . This implementation asks “Which (cell fate) identity does this specific sample have?” i.e., a multi-class classification (undifferentiated, endoderm, ectoderm, mesoderm). Please note that this is currently implemented as a beta-level feature as the number of samples for multi-class classification is relatively low. For (1), the input needs to adhere to the following guidelines: “Control” sample with ΔC_t values for all 14 genes; germ layer samples “Pluripotency”, “Endoderm”, “Ectoderm”, and “Mesoderm” with ΔC_t values for the respective 3 specific germ layer genes; and negative control sample named “a.dest” with ΔC_t values for all fourteen genes. For (2), the input needs to contain ΔC_t values for all 14 genes for each sample, and no sample should be identified as the negative control.

Data availability

The uncropped source images generated in this study have been deposited to Figshare and are available at <https://doi.org/10.6084/m9.figshare.26379658.v1>. The flow cytometry data generated in this study have been deposited to Figshare and are available at <https://doi.org/10.6084/m9.figshare.26380087.v2>. The sequencing data generated in this study have been deposited to the sequence read archive (SRA) with the BioProject accession number [PRJNA1138001](https://www.ncbi.nlm.nih.gov/bioproject/PRJNA1138001). The Biosample accession numbers of the analyzed short read-based RNAseq undifferentiated iPSCs are provided in the Source Data file. Source data are provided with this paper.

Code availability

The machine learning models and underlying training/testing data have been deposited to github and are available at <https://github.com/j-jobner/hipscore>. The hiPSCore web-tool is available as a Shiny web

application and can be accessed at <http://jdobner.shinyapps.io/hipcore>. Please contact the authors for related questions and inquiries.

References

- Kim, J. Y., Nam, Y., Rim, Y. A. & Ju, J. H. Review of the current trends in clinical trials involving induced pluripotent stem cells. *Stem Cell Rev. Rep.* **18**, 142–154 (2022).
- Liu, G., David, B. T., Trawczynski, M. & Fessler, R. G. Advances in pluripotent stem cells: history, mechanisms, technologies, and applications. *Stem Cell Rev. Rep.* **16**, 3–32 (2020).
- Takahashi, K. & Yamanaka, S. Induction of pluripotent stem cells from mouse embryonic and adult fibroblast cultures by defined factors. *Cell* **126**, 663–676 (2006).
- Takahashi, K. et al. Induction of pluripotent stem cells from adult human fibroblasts by defined factors. *Cell* **131**, 861–872 (2007).
- Moradi, S. et al. Research and therapy with induced pluripotent stem cells (iPSCs): social, legal, and ethical considerations. *Stem Cell Res. Ther.* **10**, 341 (2019).
- Hofer, M. & Lutolf, M. P. Engineering organoids. *Nat. Rev. Mater.* **6**, 402–420 (2021).
- Scudellari, M. How iPSC cells changed the world. *Nature* **534**, 310–312 (2016).
- Kim, J., Koo, B.-K. & Knoblich, J. A. Human organoids: model systems for human biology and medicine. *Nat. Rev. Mol. Cell Biol.* **21**, 571–584 (2020).
- Hirschi, K. K., Li, S. & Roy, K. Induced pluripotent stem cells for regenerative medicine. *Annu. Rev. Biomed. Eng.* **16**, 277–294 (2014).
- Pantazis, C. B. et al. A reference human induced pluripotent stem cell line for large-scale collaborative studies. *Cell Stem Cell* **29**, 1685–1702.e22 (2022).
- Dobner, J. et al. Mitochondrial DNA integrity and metabolome profile are preserved in the human induced pluripotent stem cell reference line KOLF2.1J. *Stem Cell Rep.* **19**, 343–350 (2024).
- O’Shea, O., Steeg, R., Chapman, C., Mackintosh, P. & Stacey, G. N. Development and implementation of large-scale quality control for the European bank for induced pluripotent stem cells. *Stem Cell Res.* **45**, 101773 (2020).
- Rossi, A., Lickfett, S., Martins, S. & Prigione, A. A call for consensus guidelines on monitoring the integrity of nuclear and mitochondrial genomes in human pluripotent stem cells. *Stem Cell Rep.* **17**, 707–710 (2022).
- Allison, T. F. et al. Assessment of established techniques to determine developmental and malignant potential of human pluripotent stem cells. *Nat. Commun.* **9**, 1925 (2018).
- Assou, S., Bouckenheimer, J. & De Vos, J. Concise review: assessing the genome integrity of human induced pluripotent stem cells: what quality control metrics? *Stem Cells* **36**, 814–821 (2018).
- Steichen, C., Hannoun, Z., Luce, E., Hauet, T. & Dubart-Kupferschmitt, A. Genomic integrity of human induced pluripotent stem cells: reprogramming, differentiation and applications. *World J. Stem Cells* **11**, 729–747 (2019).
- Ludwig, T. E. et al. ISSCR standards for the use of human stem cells in basic research. *Stem Cell Rep.* **18**, 1744–1752 (2023).
- Sullivan, S. et al. Quality control guidelines for clinical-grade human induced pluripotent stem cell lines. *Regen. Med.* **13**, 859–866 (2018).
- Martin, G. R. & Evans, M. J. Differentiation of clonal lines of teratocarcinoma cells: formation of embryoid bodies in vitro. *Proc. Natl. Acad. Sci. USA* **72**, 1441–1445 (1975).
- Wesselschmidt, R. L. The teratoma assay: an in vivo assessment of pluripotency. *Methods Mol. Biol.* **767**, 231–241 (2011).
- Buta, C. et al. Reconsidering pluripotency tests: do we still need teratoma assays? *Stem Cell Res.* **11**, 552–562 (2013).
- Chen, C. X.-Q. et al. A multistep workflow to evaluate newly generated iPSCs and their ability to generate different cell types. *Methods Protoc.* **4**, 50 (2021).
- Bustin, S. A. et al. The MIQE guidelines: minimum information for publication of quantitative real-time PCR experiments. *Clin. Chem.* **55**, 611–622 (2009).
- Tsankov, A. M. et al. A qPCR ScoreCard quantifies the differentiation potential of human pluripotent stem cells. *Nat. Biotechnol.* **33**, 1182–1192 (2015).
- Bock, C. et al. Reference maps of human ES and iPSC cell variation enable high-throughput characterization of pluripotent cell lines. *Cell* **144**, 439–452 (2011).
- Sato, N. et al. Molecular signature of human embryonic stem cells and its comparison with the mouse. *Dev. Biol.* **260**, 404–413 (2003).
- Ghosh, A. & Som, A. RNA-Seq analysis reveals pluripotency-associated genes and their interaction networks in human embryonic stem cells. *Comput. Biol. Chem.* **85**, 107239 (2020).
- Conesa, A. et al. A survey of best practices for RNA-seq data analysis. *Genome Biol.* **17**, 13 (2016).
- Amarasinghe, S. L. et al. Opportunities and challenges in long-read sequencing data analysis. *Genome Biol.* **21**, 30 (2020).
- Liu, L.-P. & Zheng, Y.-W. Predicting differentiation potential of human pluripotent stem cells: possibilities and challenges. *World J. Stem Cells* **11**, 375–382 (2019).
- Zhang, S. Sox2, a key factor in the regulation of pluripotency and neural differentiation. *World J. Stem Cells* **6**, 305 (2014).
- Zhang, S. et al. OCT4 and PAX6 determine the dual function of SOX2 in human ESCs as a key pluripotent or neural factor. *Stem Cell Res. Ther.* **10**, 122 (2019).
- The International Stem Cell Initiative. Characterization of human embryonic stem cell lines by the International Stem Cell Initiative. *Nat. Biotechnol.* **25**, 803–816 (2007).
- Coenye, T. Do results obtained with RNA-sequencing require independent verification? *Biofilm* **3**, 100043 (2021).
- Aguiar, V. R. C. et al. Comparison between qPCR and RNA-seq reveals challenges of quantifying HLA expression. *Immunogenetics* **75**, 249–262 (2023).
- Sloan, S. A., Andersen, J., Paşca, A. M., Birey, F. & Paşca, S. P. Generation and assembly of human brain region-specific three-dimensional cultures. *Nat. Protoc.* **13**, 2062–2085 (2018).
- No authors listed. Parkinson’s iPSC trial. *Nat. Biotechnol.* **41**, 1183 (2023).
- Müller, F.-J. et al. A bioinformatic assay for pluripotency in human cells. *Nat. Methods* **8**, 315–317 (2011).
- Lenz, M. et al. Epigenetic biomarker to support classification into pluripotent and non-pluripotent cells. *Sci. Rep.* **5**, 8973 (2015).
- Schmidt, M., Zeevaert, K., Elsafi Mabrouk, M. H., Goetzke, R. & Wagner, W. Epigenetic biomarkers to track differentiation of pluripotent stem cells. *Stem Cell Rep.* **18**, 145–158 (2023).
- Ramachandran, H., Martins, S., Kontarakis, Z., Krutmann, J. & Rossi, A. Fast but not furious: a streamlined selection method for genome-edited cells. *Life Sci. Alliance* **4**, e202101051 (2021).
- Schmid-Burgk, J. L. et al. OutKnocker: a web tool for rapid and simple genotyping of designer nuclease edited cell lines. *Genome Res.* **24**, 1719–1723 (2014).
- Zhang, M. et al. Universal cardiac induction of human pluripotent stem cells in two and three-dimensional formats: implications for in vitro maturation. *Stem Cells* **33**, 1456–1469 (2015).
- Tiwari, S. K., Wang, S., Smith, D., Carlin, A. F. & Rana, T. M. Revealing tissue-specific SARS-CoV-2 infection and host responses using human stem cell-derived lung and cerebral organoids. *Stem Cell Rep.* **16**, 437–445 (2021).
- Lu, V., Doan, M. T., Roy, I. J., Torres, A. & Teitell, M. A. Protocol for germ lineage differentiation of primed human pluripotent stem

- cells using chemically defined, nutrient-balanced media. *STAR Protoc.* **3**, 101568 (2022).
46. Graffmann, N. et al. Modeling nonalcoholic fatty liver disease with human pluripotent stem cell-derived immature hepatocyte-like cells reveals activation of PLIN2 and confirms regulatory functions of peroxisome proliferator-activated receptor alpha. *Stem Cells Dev.* **25**, 1119–1133 (2016).
47. Kuhn, M. Building predictive models in R using the caret package. *J. Stat. Softw.* **28**, 1–26 (2008).

Acknowledgements

We thank Inken Hacheney, Vanessa Baltruschat, and especially Kira Frye for excellent technical assistance. We thank Haribaskar Ramachandran for the genome editing experiments. We thank Kerstin Dobner and Leo Kurian for discussion and comments on the manuscript. The IUF is funded by the federal and state governments, the Ministry of Culture and Science of North Rhine-Westphalia (MKW), and the Federal Ministry of Education and Research (BMBF). We are grateful for the support from the Deutsche Forschungsgemeinschaft (DFG) (RO5380/1-1 to A.R. and PR1527/6-1 to A.P.), the Bundesministerium für Bildung und Forschung (BMBF) (01GM2002A to A.P.), the European Commission's Horizon Europe Programme (SIMPATRIC 101080249 to A.P.), AFM-Téléthon (AR-25179 to A.R.), and the Leibniz Competition (SAW) Cooperative Excellence project (K246/2019 to A.R. and J.K.). Figures 1–3, 6, 7 and Supplementary Figs. 11–13 contain icons generated with BioRender.

Author contributions

Conceptualization (A.R. and J.D.), methodology and source code (J.D.), investigation (J.D.), visualization (J.D.), first draft (J.D.), writing (A.R. and J.D. with the input of all authors), resources (A.R., A.P., J.K., and S.D.), supervision (A.R.), project administration, and funding acquisition (A.R., A.P., and J.K.)

Competing interests

IUF—Leibniz Research Institute for Environmental Medicine has filed a patent application for the assessment of early germ layer differentiation

capacity. J.D., J.K., and A.R. are listed as inventors. The remaining authors declare no competing interests.

Additional information

Supplementary information The online version contains supplementary material available at <https://doi.org/10.1038/s41467-024-52922-1>.

Correspondence and requests for materials should be addressed to Andrea Rossi.

Peer review information *Nature Communications* thanks the anonymous reviewer(s) for their contribution to the peer review of this work. A peer review file is available.

Reprints and permissions information is available at <http://www.nature.com/reprints>

Publisher's note Springer Nature remains neutral with regard to jurisdictional claims in published maps and institutional affiliations.

Open Access This article is licensed under a Creative Commons Attribution-NonCommercial-NoDerivatives 4.0 International License, which permits any non-commercial use, sharing, distribution and reproduction in any medium or format, as long as you give appropriate credit to the original author(s) and the source, provide a link to the Creative Commons licence, and indicate if you modified the licensed material. You do not have permission under this licence to share adapted material derived from this article or parts of it. The images or other third party material in this article are included in the article's Creative Commons licence, unless indicated otherwise in a credit line to the material. If material is not included in the article's Creative Commons licence and your intended use is not permitted by statutory regulation or exceeds the permitted use, you will need to obtain permission directly from the copyright holder. To view a copy of this licence, visit <http://creativecommons.org/licenses/by-nc-nd/4.0/>.

© The Author(s) 2024